Solvent and Substituent Effects in the Periselectivity of the Staudinger Reaction between Ketenes and α,β-Unsaturated Imines. A Theoretical and Experimental Study

Begoña Lecea,[†] Iosune Arrastia,[‡] Ana Arrieta,[‡] Guillermo Roa,[‡] Xabier Lopez,[‡] M. Isabel Arriortua,[§] Jesus M. Ugalde,[‡] and Fernando P. Cossío*,[‡]

Kimika Fakultatea, Euskal Herriko Unibertsitatea, P.K. 1072, 20080 San Sebastián-Donostia, Spain, Farmazi Fakultatea, Euskal Herriko Unibertsitatea, P.K. 450, 01080 Vitoria-Gasteiz, Spain, and Zientzi Fakultatea, Euskal Herriko Unibertsitatea, P.K. 644, E-48080 Bilbao-Bilbo, Spain

Received October 17, 1995[⊗]

The outcome of the cycloaddition between activated ketenes and α,β-unsaturated imines has been investigated both experimentally and theoretically. Our results indicate that activated monosubstituted ketenes yield exclusively [2 + 2] cycloadducts. Disubstituted activated ketenes yield [2 + 2] and/or [4 + 2] cycloadducts. In one case, an unexpected piperidin-2-one has been obtained, although its relative abundance with respect to the corresponding [2 + 2] or [4 + 2] cycloadducts can be minimized by the proper choice of experimental conditions. The ability of different *ab initio* and semiempirical methods to account for these results has been tested. The best agreement between theory and experiment is achieved at the MP2/6−31G* level of theory, with solvent effects taken into account. The semiempirical hamiltonian AM1, at the RHF level, tends to overestimate the stability of the transition structures leading to six-membered cycloadducts, whereas 3 × 3CI-HE/AM1 and CASSCF(2,2)/6−31G* methods tend to overestimate the stability and the biradical character of the transition structures leading to [2 + 2] cycloadducts.

Introduction

Ketenes exhibit a very rich cycloaddition chemistry because of their structural and electronic peculiarities.[1] In particular, these cumulenes are specially prone to [2 + 2] cycloadditions under thermal conditions.[2] Despite the formal similarity existing in the cycloaddition reaction between ketenes and double bonds, the actual mechanisms vary significantly from one system to another. Thus, [2 + 2] cycloaddition between ketenes and alkenes[3] or carbonyl compounds[4] is believed to take place in general *via* $[_\pi 2_s + _\pi 2_a]$ or $[_\pi 2_s + (_\pi 2_s + _\pi 2_s)]$ mechanisms.[5] In contrast, the reaction between ketenes and imines to yield 2-azetidinones (β-lactams), the so-called Staudinger reaction,[6] consists in a two-step mechanism,[7] in which the first step is a nucleophilic attack of the iminic nitrogen over the sp-hybridized carbon atom of the ketene to form a zwitterionic intermediate, whose conrotatory electrocyclization leads to the corresponding β-lactam (Scheme 1). This sequence of events has been studied computationally in our laboratory[8] and by other groups.[9,10] The two-step model has proved to be in agreement with the extensive experimental evidence obtained over the years.[7b,11] More recently, Hegedus[12] has shown that this model can be extended to the Staudinger reaction between imines and ketenes generated by means of photolysis of chromium carbenes.

In the case of the interaction between ketenes **1** and α,β-unsaturated imines **2**, formation of [4 + 2] and [2 + 2] cycloadducts is in principle possible (Scheme 1). According to the two-step mechanism, nucleophilic attack of **2** can lead to the zwitterionic intermediates **INTβ** and **INTδ** (see Scheme 1). Thermal electrocyclic ring closure of **INTβ** leads to the formation of β-lactams **3**, whereas the six-electron disrotatory thermal electrocyclization of **INTδ** should lead to δ-lactams (3,4-dihydro-2-pyridones)

[†] Farmazi Fakultatea.
[‡] Kimika Fakultatea.
[§] Zientzi Fakultatea.
[⊗] Abstract published in *Advance ACS Abstracts,* April 1, 1996.

(1) Tidwell, T. T. *Ketenes*; Wiley: New York, 1995; pp 459−571.
(2) (a) Woodward, R. B.; Hoffmann, R. *The Conservation of Orbital Symmetry*; Verlag Press: New York, 1969. (b) Houk, K. N.; Strozier, R. W.; Hall, J. A. *Tetrahedron Lett.* **1974**, 897. (c) Ghosez, L.; O'Donnell, M. J. *Pericyclic Reactions*; Marchand, A. P., Lehr, R. E., Eds.; Academic Press: New York, 1977; Vol. 3, pp 79−140.
(3) (a) Valentí, E.; Pericàs, M. A.; Moyano, A. *J. Org. Chem.* **1990**, *55*, 3582. (b) Wang, X.; Houk, K. N. *J. Am. Chem. Soc.* **1990**, *112*, 1754. (c) Yamabe, S.; Minato, T.; Osamura, Y. *J. Chem. Soc., Chem. Commun.* **1993**, 450. For stepwise reaction paths see ref 3a and: (d) Bernardi, F.; Bottoni, A.; Robb, M. A.; Venturini, A. *J. Am. Chem. Soc.* **1990**, *112*, 2106.
(4) (a) Lecea, B.; Arrieta, A.; Roa, G.; Ugalde, J. M.; Cossío, F. P. *J. Am. Chem. Soc.* **1994**, *116*, 9613. (b) Krabbenhoft, H. O. *J. Org. Chem.* **1978**, *43*, 1305.
(5) (a) Baldwin, J. E.; Kapecki, J. A. *J. Am. Chem. Soc.* **1970**, *92*, 4874. (b) Pasto, D. J. *J. Am. Chem. Soc.* **1979**, *101*, 37.
(6) Staudinger, H. *Liebigs Ann.Chem.* **1907**, *356*, 51.
(7) (a) Hegedus, L. S.; Montgomery, J.; Narukawa, Y.; Snustad, D. C. *J. Am. Chem. Soc.* **1991**, *113*, 5784. (b) Georg, G. L.; Ravikumar, V. T. In *The Organic Chemistry of β-Lactams*; Georg, G. L., Ed.; Verlag Chemie: New York, 1993; pp 295−381.
(8) (a) Cossío, F. P.; Ugalde, J. M.; Lopez, X.; Lecea, B.; Palomo, C. *J. Am. Chem. Soc.* **1993**, *115*, 995. (b) Cossío, F. P.; Arrieta, A.; Lecea, B.; Ugalde, J. M. *J. Am. Chem. Soc.* **1994**, *116*, 2085. (c) Arrieta, A.; Ugalde, J. M.; Cossío, F. P.; Lecea, B. *Tetrahedron Lett.* **1994**, *35*, 4465. (d) Arrastia, I.; Arrieta, A.; Ugalde, J. M.; Cossío, F. P., Lecea, B. *Tetrahedron Lett.* **1994**, *35*, 7825.
(9) (a) Sordo, J. A.; González, J.; Sordo, T. L. *J. Am. Chem. Soc.* **1992**, *114*, 6249. (b) López, R.; Sordo, T. L.; Sordo, J. A.; González, J. *J. Org. Chem.* **1993**, *58*, 7036. (c) Assfeld, X.; Sordo, J. A.; González, J.; Ruiz-López, M. F.; Sordo, T. L. *THEOCHEM* **1993**, *287*, 193. (d) Assfeld, X.; Ruiz-López; M. F.; ; González, J.; López, R.; Sordo, J. A.; Sordo, T. L. *J. Comput.Chem.* **1994**, *15*, 479.
(10) (a) Boyd, D. B. *Computer-Assisted Molecular Design Studies of β-Lactam Antibiotics*. In *Frontiers on Antibiotic Research*; Umezawa, H., Ed.; Academic Press: Tokyo, 1987; pp 339−356. (b) Cooper, R. D. G.; Daugherty, B. W.; Boyd, D. B. *Pure Appl. Chem.* **1987**, *59*, 485.
(11) (a) Ghosez, L.; Marchand-Brynaert, J. In *Comprehensive Organic Synthesis*; Trost, B., Fleming, I., Eds.; Pergamon: Oxford, 1991; Vol. 5, pp 85−122. (b) Thomas, R. C. In *Recent Progress in the Chemical Synthesis of Antibiotics*; Lukacs, G., Ohno, M., Eds.; Springer-Verlag: Berlin, 1989; p 533. (c) Van der Steen, F. H.; Van Koten, G. *Tetrahedron* **1991**, *47*, 7503. (d) Backes, I. In *Methoden der Organischen Chemie*; Kalgman, D., Ed.; Georg Thieme: Stuttgart, 1991; Vol. E15b, Organische Stickstoffverbindungen II, pp 383−483. (e) Oligaruso, M. A.; Wolfe, J. F. In *Synthesis of Lactones-Updates from the Chemistry of Functional Groups*; Patai, S., Rappoport, Z., Eds.; Wiley: Chichester, 1993; pp 168−268 and 490−623.
(12) Dumas, S.; Hegedus, L. S. *J. Org. Chem.* **1994**, *59*, 4967.

S0022-3263(95)01867-6 CCC: $12.00

Scheme I[a]

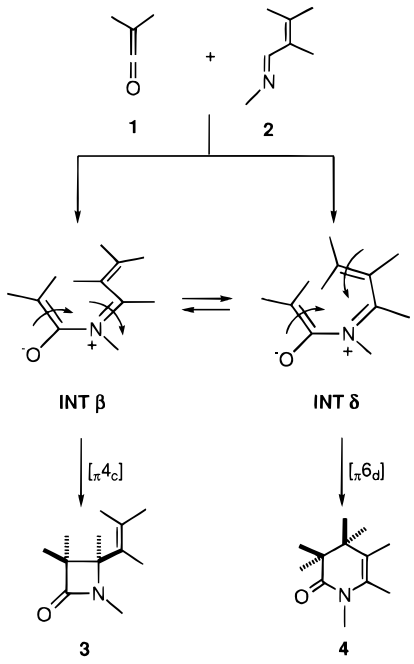

[a] The possible substituents at the different positions are not specified.

4. Both types of cycloadducts have been found experimentally,[8−22] depending upon the nature of the substituents incorporated at the different positions of the reactants **1** and **2**.

The periselectivity of the reaction between ketenes and α,β-unsaturated imines is relevant not only from a theoretical standpoint but also from a practical perspective, since β-lactams of type **3** are important building blocks in the chemical synthesis of β-lactam antibiotics.[23] In effect, oxidative cleavage of the exocyclic double bond of **3** and ulterior elaboration leads to formation of bicyclic β-lactams of biological interest, in particular carbapenem compounds.[24] Therefore, a satisfactory understanding of the factors leading to formation of cycloadducts **3** instead of δ-lactams **4** is highly desirable.

In a recent preliminary paper,[8d] we have reported that cycloaddition between a monosubstituted ketene such as methoxyketene and (*E*)-*N*-(α-methylcinnamylidene)-methylamine yields exclusively the corresponding [2 + 2] cycloadduct and that semiempirical calculations must be performed at a configuration interaction level of theory in order to correctly reproduce the observed periselectivity of the reaction. This preliminary study suggested that the energy gap between the reaction paths leading to the [2 + 2] and [2 + 4] cycloadducts could be reduced using disubstituted ketenes, thus reversing the periselectivity of the reaction. Bearing in mind preliminary results, and in connection with the precedents exposed above, the aim of the present work has been to study the periselectivity of the cycloaddition between ketenes and α,β-unsaturated imines (1-aza dienes), taking into account both solvent and substituent effects, in order to develop a general model which could explain the variables governing the formation of [2 + 2] and [4 + 2] cycloadducts.

Computational Methods

Semiempirical calculations have been carried out with the AM1[25] Hamiltonian with the standard parameters,[25,26] as implemented in the MOPAC 6.0 package.[27] The molecular mechanics correction for the amidic bonds was not used.[8a,b] Stationary points were located using the NLLSQ[28] and eigenvector following[29] algorithms. All stationary points were refined by minimization of the gradient norm of the energy at least below 0.01 kcal/Å deg and with 2 orders of magnitude tighter SCF convergence criteria, as recommended by Boyd, Stewart, *et al.*[30] These calculations were performed at both the RHF and 3 × 3 configuration interaction−half-electron (3 × 3CI-HE) levels.[31] The choice of these particular semiempirical methods and options is based upon our previous experience in the Staudinger reaction between ketenes and imines.[8]

All *ab initio* calculations performed in this work have been carried out using the GAUSSIAN 92,[32] GAUSSIAN 92/DFT,[33] and GAMESS[34] packages, with either 3−21G and 6−31G* basis sets.[35] Single-point energy calculations, as well as geometry optimizations and subsequent frequency calculations,[36] were carried out with the RHF, the multiconfigurational complete active space-SCF (CASSCF),[37] and the density functional theory (DFT)[38] methodologies. MP2/6−31G* calculations[39] were also performed, using the corresponding RHF geometries and

(13) Pfleger, R.; Jäger, A. *Chem. Ber.* **1957**, *90*, 2460.
(14) Hull, R. *J. Chem. Soc. C* **1967**, 1154.
(15) Gompper, R. *Angew. Chem., Int. Ed. Engl.* **1969**, *8*, 312.
(16) Duran, F.; Ghosez, L. *Tetrahedron Lett.* **1970**, 245.
(17) Sakamoto, M.; Tomimatsu, Y. *Yakugaku Zasshi* **1970**, *90*, 1386; C. A.
(18) Komatsu, M.; Yamamoto, S.; Ohshiro, Y.; Agawa, T. *Tetrahedron Lett.* **1981**, *22*, 3769 and ref 4 and 5 therein.
(19) Moore, H. W.; Hughes, G. *Tetrahedron Lett.* **1982**, *23*, 4003.
(20) Brady, W. T.; Shiem, C. H. *J. Org. Chem.* **1983**, *48*, 2499.
(21) Moore, H. W.; Hughes, G.; Srinivasachar, K.; Fernandez, M.; Nguyen, N. V.; Schoon, D.; Tranne, A. *J. Org. Chem.* **1985**, *50*, 4231.
(22) Palomo, C.; Cossío, F. P.; Odriozola, J. M.; Oiarbide, M.; Ontoria, J. M. *J. Org. Chem.* **1991**, *56*, 4418.
(23) *Chemistry and Biology of β-Lactam Antibiotics*; Morin, R. B., Gorman, M., Eds.; Academic Press: New York, 1982; Vols. 1−3.
(24) Kant, J.; Walker, D. G. In *The Organic Chemistry of β-Lactams*; Georg, G. I., Ed.; Verlag Chemie: New York, 1993; pp 121−196.
(25) Dewar, M. J. S.; Zoebisch, E. G.; Healy, E. F.; Stewart, J. J. P. *J. Am. Chem. Soc.* **1985**, *107*, 3902.
(26) Dewar, M. J. S.; Zoebisch, E. G. *THEOCHEM* **1988**, *180*, 1.
(27) (a) Stewart, J. J. P. *QCPE Bull.* **1983**, *3*, 101. (b) *QCPE No. 455*; Indiana University, Bloomington, IN.
(28) Bartels, R. H. Report CNA-44; University of Texas; Center for Numerical Analysis: Austin, TX, 1972.
(29) Baker, J. *J. Comput. Chem.* **1986**, *7*, 385.
(30) Boyd, D. B.; Smith, D. W.; Stewart, J. J. P.; Wimmer, E. *J. Comput. Chem.* **1988**, *9*, 387.
(31) (a) Dewar, M. J. S.; Hashnall, J. A.; Venier, C. G. *J. Am. Chem. Soc.* **1968**, *90*, 1953. (b) Dewar, M. J. S.; Olivella, S. *J. Chem. Soc., Faraday Trans. 2* **1979**, *75*, 829. (c) Salem, L. *Pure Appl. Chem.* **1973**, *33*, 317.
(32) Gaussian 92, Revision C: Frisch, M. J.; Trucks, G. W.; Head-Gordon, M.; Gill, P. M. W.; Wong, M. W.; Foresman, J. B.; Johnson, B. G.; Schlegel, H. B.; Robb, M. A.; Replogle, E. S.; Gomperts, R.; Andres, J. L.; Raghavachari, K.; Binkley, J. S.; Gonzalez, C.; Martin, R. L.; Fox, D. J.; Defrees, D. J.; Baker, J.; Stewart, J. J. P.; Pople, J. A. Gaussian, Inc., Pittsburgh, PA, 1992.
(33) Gaussian 92/DFT, revision F.4: Frisch, M. J.; Trucks, G. W.; Schlegel, H. B.; Gill, P. M. W.; Johnson, B. G.; Wong, M. W.; Foresman, J. B.; Robb, M. A.; Head-Gordon, M.; Replogle, E. S.; Gomperts, R.; Andres, J. L.; Raghavachari, K.; Binkley, J. S.; Gonzalez, C.; Martin, R. L.; Fox, D. J.; Defrees, D. J.; Baker, J.; Stewart, J. J.P.; Pople, J. A., Gaussian, Inc., Pittsburgh PA, 1993.
(34) GAMESS (General Atomic and Molecular Electronic Structure System, CRAY-UNICOS Version). (a) Schmidt, M. W.; Baldridge, K. K.; Boatz, J. A.; Jensen, J. M.; Koseki, S.; Gordon, M. S.; Nguyen, K. A.; Windus, T. L.; Elbert, S. T. *QCPE Bull.* **1990**, *10*, 52. (b) Schmidt, M. W.; Baldridge, K. K.; Boatz, J. A.; Gordon, M. S.; Jensen, J. M.; Koseki, S.; Matsunaga, N.; Nguyen, K. A.; Su, S.; Windus, T. L. *J. Comput. Chem.* **1993**, *14*, 1347.
(35) Hehre, W. J.; Radom, L.; Schleyer, P.v.R.; Pople, J. A. *Ab Initio Molecular Orbital Theory*; Wiley: New York, 1986; pp 65−88 and references therein.
(36) McIver, J. W.; Komornicki, A. *J. Am. Chem. Soc.* **1972**, *94*, 2625.
(37) Roos, B. O.; Taylor, P. R.; Siegbahn, P. E. M. *Chem. Phys.* **1980**, *48*, 157.

keeping the core electrons frozen. Approximate DFT calculations were carried out using an hybrid three-parameter functional developed by Becke,[40] which combines the Becke's gradient corrected exchange functional and the Lee−Yang−Parr and Vosko−Wilk−Nusair correlation functionals[41] with part of the exact Hartree−Fock exchange energy.

Ruiz-López *et al.*[9c] have pointed out the importance of solvent effects on the mechanism of the Staudinger reaction. In view of this, we have also optimized some of the relevant stationary points using a relatively simple self-consistent reaction field (SCRF)[42] method, based on the Onsager model,[43] in which the solvation energy is calculated from the electrostatic energy between the solute, modelized as a dielectric sphere of radius a_o, and the solvent, described as a continuum of electric permitivity ϵ. The solvent considered in the calculations and used in the experimental work is dichloromethane (ϵ = 9.08).

Results and Discussion

General Considerations. Given the combined experimental and computational character of our investigation, we first chose substrates possessing a readily verifiable stereochemistry, both in the reactants and in the products. In addition, we selected the starting materials **1** and **2** as simple as possible, in order to restrict reasonably the degrees of freedom of the species considered and facilitate accordingly the computation of the diverse reaction paths. Figure 1 shows the ketenes and imines included in our study, as well as the possible cycloadducts formed. Given the instability of ketenes, especially the activated ones, the cumulenes **1c**−**e** were generated *in situ* by means of dehydrohalogenation of the corresponding acyl chlorides **1′c**−**e** in the presence of triethylamine.[44] This experimental approach is valid, since Lynch *et al.*[45] proved that in the reaction of acyl chlorides and imines in the presence of a tertiary base the ketene is formed prior to the cycloaddition stages. Apart from ketene (**1a**) itself, we selected methoxyketene (**1c**) and chloroketene (**1d**) as model activated monosubstituted ketenes. Chloromethylketene (**1e**) and dichloroketene (**1f**) were included as model disubstituted ketenes. For the computational part of our study, we considered in the semiempirical calculations stationary points derived from the reaction of ketenes **1a**−**f**, whereas in the *ab initio* calculations only ketenes **1a,b** and **1d**−**f** were considered. With respect to the α,β-unsaturated imines, 1-azadienes **2b,c** give a good compromise between structural simplicity and stability.

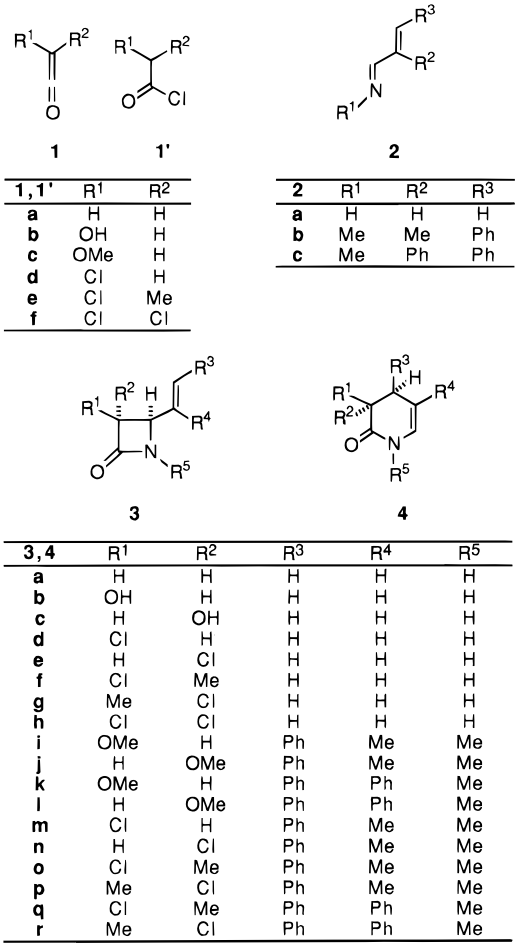

1,1'	R^1	R^2
a	H	H
b	OH	H
c	OMe	H
d	Cl	H
e	Cl	Me
f	Cl	Cl

2	R^1	R^2	R^3
a	H	H	H
b	Me	Me	Ph
c	Me	Ph	Ph

3,4	R^1	R^2	R^3	R^4	R^5
a	H	H	H	H	H
b	OH	H	H	H	H
c	H	OH	H	H	H
d	Cl	H	H	H	H
e	H	Cl	H	H	H
f	Cl	Me	H	H	H
g	Me	Cl	H	H	H
h	Cl	Cl	H	H	H
i	OMe	H	Ph	Me	Me
j	H	OMe	Ph	Me	Me
k	OMe	H	Ph	Ph	Me
l	H	OMe	Ph	Ph	Me
m	Cl	H	Ph	Me	Me
n	H	Cl	Ph	Me	Me
o	Cl	Me	Ph	Me	Me
p	Me	Cl	Ph	Me	Me
q	Cl	Me	Ph	Ph	Me
r	Me	Cl	Ph	Ph	Me

Figure 1. Substrates and cycloadducts studied in this work.

Experimental Results

Since it seems likely that the periselectivity of the Staudinger reaction was sensitive to substituent effects, we checked experimentally the reactivity of imines **2b,c** toward ketenes **1c**−**e**.

We first prepared imines **2b,c** by means of the condensation between *in situ* generated methylamine and α-methyl, and α-phenylcinnamaldehyde, respectively (Scheme 2). The (*E*)-configuration of the iminic C=N bond was verified *via* NOE experiments, presaturating the ^{1}H-NMR signal corresponding to the *N*-methyl groups of **2b,c** and observing a significant NOE (11−14%) in the signal associated with the iminic HC=N protons. An excess of methyl amine hydrochloride was necessary to achieve conversions of *ca.* 85%. The crude imines thus obtained were contaminated by the starting aldehyde (see the supporting information). Attempts to purify **2b,c** by flash chromatography resulted in decomposition of the imines. On the other hand, distillation of the crude imines under reduced pressure resulted in their partial isomerization around the C=C bonds to yield mixtures of **2b,c** and their stereoisomers **2′b,c**, the corresponding ratios being 6:1 and 4:1 for **2b**:**2b′** and **2c**:**2c′**, respectively. The structural elucidation of these latter compounds will be discussed later. Since these aldehydes do not react under the conditions required to form lactams, the crude imines **2b,c** were used as such in the cycloaddition reactions.

(38) Parr, R. G.; Yang, W. *Density-Functional Theory of Atoms and Molecules*; Oxford: New York, 1989.
(39) (a) Binkley, J. S.; Pople, J. A. *Int. J. Quantum Chem.* **1975**, *9*, 229. (b) Pople, J. A.; Binkley, J. S.; Seeger, R. *Int. J. Quantum Chem. Symp.* **1976**, *10*, 1.
(40) Becke, A. D. *J. Chem. Phys.* **1993**, *98*, 5648.
(41) (a) Becke, A. D. *Phys. Rev. A* **1988**, *38*, 3098. (b) Lee, C.; Yang, W.; Parr, R. G. *Phys. Rev. B* **1980**, *37*, 785. (c) Vosko, S. H.; Wilk, L.; Nusair, M. *Can. J. Phys.* **1980**, *58*, 1200.
(42) (a) Tomasi, J.; Persico, M. *Chem. Rev.* **1974**, *94*, 2027. (b) Simkin, B. Ya.; Sheikhet, I. *Quantum Chemical and Statistical Theory of Solutions—A Computational Approach*; Ellis Horwood: London, 1995; pp 78−101.
(43) (a) Wong, M. W.; Frisch, M. J.; Wiberg, K. B. *J. Am. Chem. Soc.* **1990**, *112*, 4776. (b) Wong, M. W.; Wiberg, K. B.; Frisch, M. J. *J. Chem. Phys.* **1991**, *95*, 8991.
(44) (a) Sheehan, J. C.; Ryan, J. J. *J. Am. Chem. Soc.* **1951**, *73*, 1204. (b) Manhas, M. S.; Chib, J. S.; Chiang, Y. H.; Bose, A. K. *Tetrahedron* **1969**, *25*, 4421.
(45) Lynch, J. E.; Riseman, S. M.; Laswell, W. L.; Tschaen, D. M.; Volante, R. P.; Smith, G. B.; Shinkai, I. *J. Org. Chem.* **1989**, *54*, 3792.

Scheme 2[a,b]

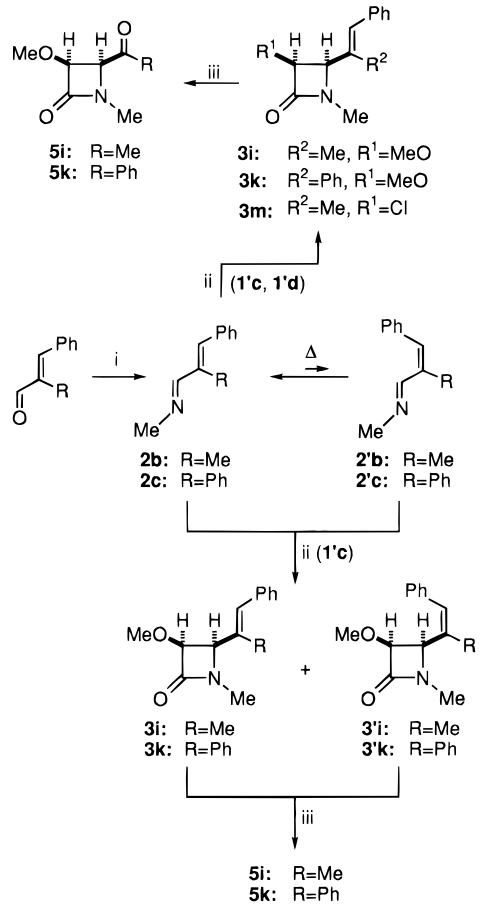

[a] Only one enantiomer is drawn for all chiral compounds. [b] Reagents and conditions: (i) $MeNH_3^+Cl^-$, NEt_3, CH_2Cl_2, $MgSO_4$, rt; (ii) **1′**, NEt_3, CH_2Cl_2, −78 °C → rt; (iii) $KMnO_4$, Me_2CO-H_2O, reflux.

Reaction between imine **2b** and ketenes **1c** and **1d** led to the exclusive formation of the [2 + 2] cycloadducts **3i** and **3m**. Similarly, the imine **2c**, when reacted with ketene **1c**, was transformed into the *β*-lactam **3k** (see Scheme 2). The structure of cycloadducts **3i,m,k** was unequivocally established on the basis of their IR spectra. Thus, all of these strained compounds exhibit strong IR bands in the range 1753−1766 cm^{-1}, corresponding to absorption of *β*-lactam carbonyl groups.[46] The stereochemistry was established by measuring the coupling constants corresponding to the signals of the C(3)-H and C(4)-H methines. The values of $^3J_{3,4}$ obtained lie in the range of 4.6−4.8 Hz, thus indicating a *cis* configuration.[47] The structure of *β*-lactams **3i,k** was further confirmed by oxidation of the exocyclic double bond to yield the 4-acyl *β*-lactams **5i,k**. These compounds exhibit two carbonyl absorptions in their IR spectra, one of them being of *ca.* 1750 cm^{-1}, whereas the other lies in the range of 1683−1718 cm^{-1}. These IR bands were assigned to the *β*-lactam and ketone carbonyls, respectively.

When the mixtures of imines **2b,c** and **2′b,c** were subjected to the Staudinger reaction in the presence of methoxyacetyl chloride (**1′c**) and triethylamine, two [2 + 2] cycloadducts **3i,k** and **3′i,k** were obtained in the same ratios as those observed in the starting imines. The structural assignation of **3′i,k** was established on the basis of oxidation experiments (see Scheme 2).

Scheme 3[a,b]

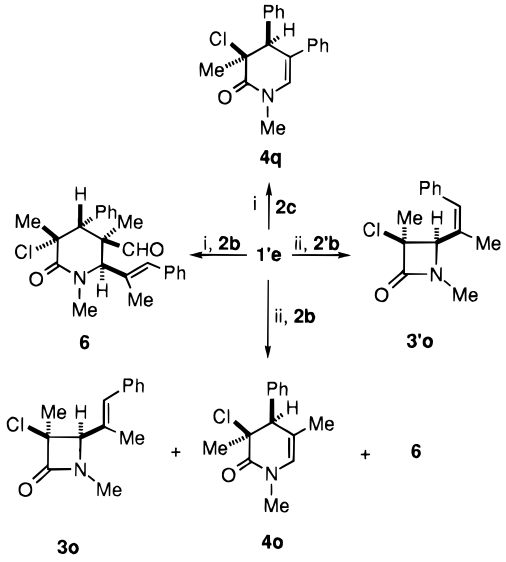

[a] Only one enantiomer is drawn for all chiral compounds. [b] Reagents and conditions: (i) NEt_3 (1.5 equiv), CH_2Cl_2, −78 °C → rt, slow addition of **1′e** over **2b** in NEt_3; (ii) NEt_3 (1.5 equiv), CH_2Cl_2, −78 °C → rt, slow addition of NEt_3 over **1′e** at −78 °C, followed by slow addition of a diluted solution of **2b** or **2′b** at −78 °C (see the Experimental Section for details).

These data are in agreement with the experimental evidence available for the cycloaddition between monosubstituted ketenes[48] (as well as ketene[49] itself) and α,*β*-unsaturated imines. The case of ketene is controversial, since an early paper[13] claimed that the reaction between ketene and cinnamylideneaniline yields the corresponding [4 + 2] product. This result was reinvestigated by Kato *et al.*,[49] who demonstrated that the reaction of gaseous ketene with cinnamylidene aniline at 180−200 °C yields exclusively the [2 + 2] cycloadduct.

Once we have verified that (*E*)-imines **2b,c** do not exhibit untypical behavior toward monosubstituted ketenes (apart from the thermal isomerization around the C=C bond), we checked their reactivity toward chloromethylketene **1e**. We have found that reaction of **1e** with imine **2c** exclusively yields the [4 + 2] cycloadduct **4q** (Scheme 3). Its structure was unequivocally established on the basis of the ^{1}H-NMR and ^{13}C-NMR spectra, as well as by IR spectroscopy. Thus, the stretching vibration of the carbonyl group of **4q** was observed at 1674 cm^{-1}, a normal value for nonstrained lactams. The *cis* relationship between the methyl group at C(3) and the methinic proton at C(4) was confirmed by a NOE experiment performed presaturating the resonance of the

(46) Bose, A. K.; Manhas, M. S.; Van der Veen, J. M.; Amin, S. G.; Fernandez, I. F.; Gala, K.; Gruska, R.; Kapur, J. C.; Khajavi, M. S.; Kreder, J.; Mukkavilli, L.; Ram, B.; Sugiura, M.; Vincent, J. E. *Tetrahedron* **1981**, *37*, 2321.

(47) Kagan, H. B.; Basselier, J. J.; Luche, J. L. *Tetrahedron Lett.* **1964**, 941.

(48) For significant examples, see: (a) Dugat, D.; Just, G.; Sahoo, S. *Can. J. Chem.* **1987**, *65*, 88. (b) Zamboni, R.; Just, G. *Can. J. Chem.* **1979**, *57*, 1945. (c) Kronenthal, D. R.; Han, C. Y.; Taylor, M. K. *J. Org. Chem.* **1982**, *47*, 2765. (d) Evans, D. E.; Sjögren, E. B. *Tetrahedron Lett.* **1985**, *26*, 3783. (e) Ikota, N.; Hanaki, A. *Heterocycles* **1984**, *22*, 2227. (f) Ikota, N. *Chem. Pharm. Bull.* **1990**, *38*, 1601. (g) Borer, B. C.; Balogh, D. W. *Tetrahedron Lett.* **1991**, *32*, 1039. (h) Georg, G. I.; Akgün, E.; Mashava, P.; Milstead, M.; He, P.; Wu, Z.; Velde, D. V.; Takusagawa, F. *Tetrahedron Lett.* **1992**, *33*, 2111. (i) Georg, G. I.; Mashava, P. M.; Guan, X. *Tetrahedron Lett.* **1991**, *32*, 581. (j) Gunda, T. E.; Vieth, S.; Kover, K. E.; Sztaricskkai, F. *Tetrahedron Lett.* **1990**, *31*, 6707.

(49) Katagiri, N.; Miura, R.; Niwa, R.; Kato, T. *Chem. Pharm. Bull.* **1983**, *31*, 538.

methyl group. When we carried out the reaction with imine **2b** and ketene **1e** under the same reaction conditions (method A, see the Experimental Section), we obtained a sole product whose spectral and microanalytical properties were incompatible with those expected for the "normal" cycloadducts **3o** or **4o**. Fortunately, good quality crystals of this unexpected compound could be obtained. Much to our surprise, the structure of this compound was found to be that reported in Scheme 3 and in Figure 1 of the supporting information. Attempts to generalize this anomalous reaction were unsuccessful. We reasoned[50] that formation of **6** is favored when the reaction is carried out under conditions in which the ketene is in the presence of an excess of imine. Thus, we repeated the experiment under the reaction conditions specified in method B of the Experimental Section. In this latter protocol, not only the sequence of addition of the reagents is reversed, but also the reaction was diluted 5-fold with respect to the previous experiment, in order to favor bimolecular reactions instead of the trimolecular process. Under these conditions, compound **6** was formed in only 2% yield, and [4 + 2] and [2 + 2] lactams **4o** and **3o** were obtained in 7% and 16% yields, respectively. It is noteworthy that, when a mixture of imines **2b** and **2′b** was allowed to react with ketene **1e** under these latter conditions, compounds **3o**, **4o**, and **6** were obtained in the same ratio, together with a 6% yield of β-lactam **3′o**. Therefore, we concluded that imine **2′b** yields exclusively the corresponding [2 + 2] cycloadduct **3′o**, thus proving that the periselectivity of the reaction is sensitive to the substitution of the β position of the α,β-unsaturated imine.

To summarize our experimental studies and the precedents commented above, we can conclude that: (i) monosubstituted ketenes and ketene itself yield [2 + 2] cycloadducts when reacted with α,β-unsaturated imines. (ii) Under the same conditions, disubstituted activated ketenes with alkyl groups[19−22] form either [4 + 2] or [2 + 2] cycloadducts. In general, dichloroketene forms exclusively [4 + 2] cycloadducts.[16,20]

Computational Results

Previous computational studies performed in our laboratory[8] have shown that the stereoselectivity of the Staudinger reaction is not determined by the first step, *i.e.*, the formation of the N(1)−C(2) bond, but by the electrocyclization step leading to the formation of the C(3)−C(4) bond. In the case of the Staudinger reaction between ketenes and α,β-unsaturated imines, we have also found[8d] that interconversion between the zwitterionic intermediates **INTβ** and **INTδ** is facile and therefore the periselectivity of the reaction is determined by the relative energies of the TS's corresponding to the thermal conrotatory or disrotatory electrocyclization of **INTβ** or **INTδ**, respectively (see Scheme 1). We have denoted these TS's as **TSβ** and **TSδ**, and their general shape is depicted in Figure 2. It is noteworthy that both TS's adopt nonplanar conformations, in order to minimize the torsion around the π-systems present in intermediates **INTβ** and **INTδ**. We[8] and others[9] have also shown that saddle points like **TSβ** are sensitive to torquoelectronic effects. According to this concept introduced by Houk,[51] substituents possessing donor character "prefer" to occupy *outward* positions. It is important to note that, in the case of **TSβ** saddle points, the 4-vinyl groups are necessarily in a *4-inward* disposition, provided that the starting α,β-unsaturated imine had a (*E*)-stereochemistry. In our NOE experiments with imines **2b,c** we have explicitly shown that this is indeed the case, so only **TSβ** saddle points with *inward* vinyl groups at C(4) have been considered. This allows the substituent (or substituents) of the ketene moiety to adopt either *3-inward* or *3-outward* dispositions. Therefore, both possibilities have been considered for the interaction between (*E*)-α,β-unsaturated imines and unsymmetrically substituted ketenes. We have also computed transition structures of the type **TSδ**, leading to [4 + 2] cycloadducts. In principle, for a given α,β-unsaturated imine, the two substituents present in the starting ketene can occupy either the *3-inward* or the *3-outward* positions, as in the preceding case (see Figure 2). In addition, the (*E*)-geometry usually present in the vinylic moieties of imines **2b,c** implies that the substituents R^3 in Figure 2 must necessarily be in a *4-outward* disposition.

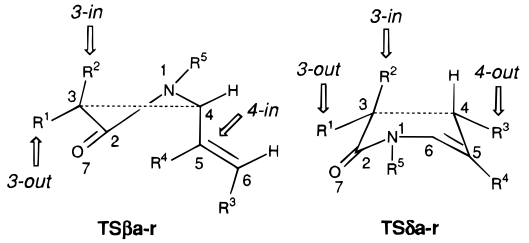

Figure 2. General features of transition structures leading to [2 + 2] and [4 + 2] cycloadducts (**TSβa−r** and **TSδa−r**), respectively. The substitution patterns are the same as indicated in Figure 1 for cycloadducts **3** and *4*.

We have computed the structures and the energies of the saddle points **TSβa−r** and **TSδa−r**, corresponding to simple representative structures and to the compounds studied experimentally in the previous section. First, we have used the AM1 semiempirical Hamiltonian in view of its reasonable computational cost and because we have previously found[8] that it describes accurately enough the main variables governing the Staudinger reaction. The heats of formation of saddle points **TSβa−r** and **TSδa−r**

(50) A possible rationalization of the formation of compound **6** is as follows:

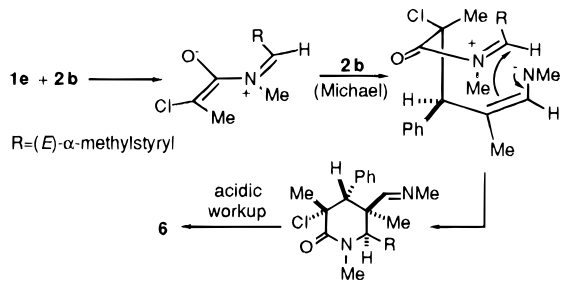

This sequence of events is supported by the fact that reaction of a 1:1:1 mixture of **1c**, **2b**, and *(E)*-α-methylcinnamaldehyde does not improve the yield of **6**. On the other hand, formation of the proposed intermediate imine has been detected by ^{1}H-NMR of the crude reaction mixture before the usual acidic workup.

(51) (a) Kirmse, W.; Rondan, N. G.; Houk, K. N. *J. Am. Chem. Soc.* **1984**, *106*, 1989. (b) Houk, K. N.; Rondan, N. G. *J. Am. Chem. Soc.* **1985**, *107*, 2099. (c) Rudolf, K.; Spellmeyer, D. C.; Houk, K. N. *J. Org. Chem.* **1987**, *52*, 3708. (d) Houk, K. N.; Spellmeyer, D. C.; Jefford, Ch.W.; Rimbault, C. G.; Wang, Y.; Miller, R. D. *J. Org. Chem.* **1988**, *53*, 2125. (e) Buda, A. B.; Wang, Y.; Houk, K. N. *J. Org. Chem.* **1989**, *54*, 2264. (f) Jefford, Ch.W.; Bernardinelli, G.; Wang, Y.; Spellmeyer, D. C.; Buda, A.; Houk, K. N. *J. Am. Chem. Soc.* **1992**, *114*, 1157. (g) Niwayama, S.; Houk, K. N. *Tetrahedron Lett.* **1993**, *34*, 1251. (h) Nakamura, K. Houk, K. N. *J. Org. Chem.* **1995**, *60*, 686.

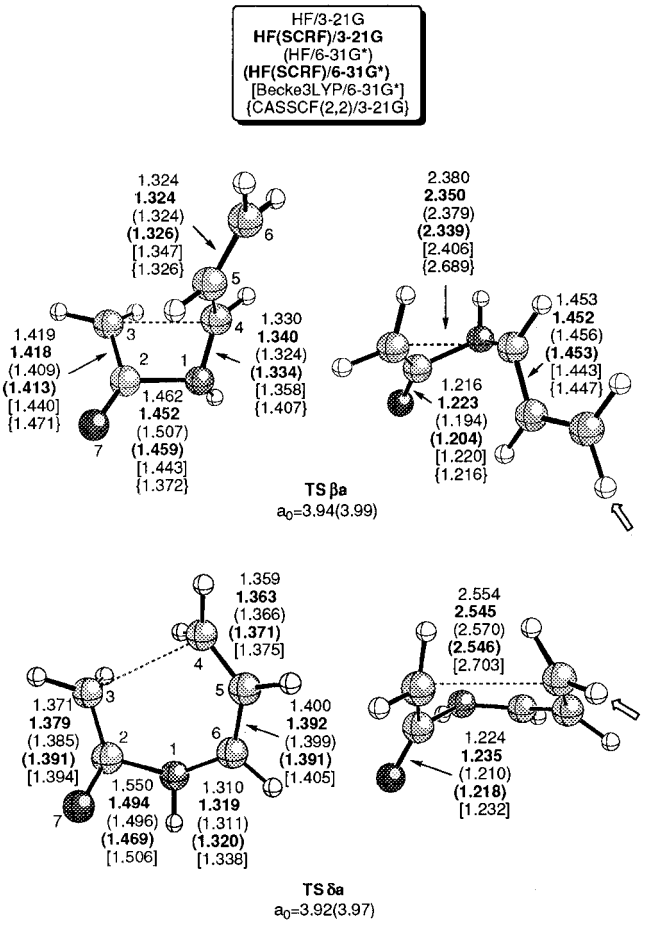

Figure 3. Computer plots of saddle points **TS*β*a** and **TS*δ*a**, calculated at different theoretical levels, a_o values correspond to the spherical cavity radii. In this and the following figures which incorporate ball-and-stick representations, unless otherwise noted, atoms are represented by increasing order of shading as follows: H, C, N, O. Distances and angles are given in Å and deg, respectively.

(see Figures 1 and 2) as well as their C(3)−C(4) bond distances are collected in Table 1 of the supporting information. From the data collected in this table we can observe that the RHF/AM1 method predicts that saddle points **TS*β*** are always more energetic than their **TS*δ*** analogs, with an average difference in enthalpy of *ca.* 5.8 kcal/mol. By contrast, the 3 × 3CI-HE/AM1 method predicts that saddle points **TS*β*** are always *less* energetic than their **TS*δ*** analogs, the average difference in enthalpies being *ca.* 3.8 kcal/mol. This can be explained by taking into account that the 3 × 3CI-HE/AM1 method assigns a larger biradical character to **TS*β*** saddle points than to their corresponding **TS*δ*** analogs, along with the well-known tendency of semiempirical methods to overestimate the stability of biradicals at both UHF and 3 × 3CI-HE levels.[52] Therefore, the semiempirical method AM1, although useful in the elucidation of other features of the Staudinger reaction, is not accurate enough to predict its periselectivity. In view of this result, we directed our attention to *ab initio* methods.

We studied first the geometrical and energetic features of the transition structures corresponding to the reaction between the simplest partners, *i.e.*, ketene **1a** and vinylideneamine **2a.** We have located and characterized the saddle points **TS*β*a** and **TS*δ*a** leading to the formation of 4-vinylazetidin-2-one (**3a**) and 3,4-dihydropyridin-2-one **4a**, respectively. The chief geometrical features of both TS's at different levels of theory and with two split-valence basis sets are reported in Figure 3. From the data collected in Figure 3 we can observe that the geometries obtained at the HF/3−21G and HF/6−31G* levels are very similar. In the case of **TS*β*a**, the C(3)−C(4) distances at both levels are slightly lower when solvent effects are included. This distance is increased when electron correlation is included in the course of the optimization (see the Becke3LYP/6−31G* results). Finally, the largest value is found at the CASSCF(2,2)/3−21G level. It is noteworthy that the two natural orbitals σ_{34} and σ^*_{34} included in the active space of the CASSCF calculation have occupancies of 1.425 and 0.575, respectively, which are customary regarded as suggestive of significant biradicaloid character.[53,54]

The geometrical features of **TS*δ*a** are also collected in Figure 3. At all the levels studied, we have found that this saddle point is earlier than **TS*β*a**. Thus, the C(3)−C(4) distances are larger than those previously obtained, whereas the C(2)−C(3) distances are shorter. Again, we have found that the HF/3−21G and HF/6−31G* are very similar and that the SCRF data correspond to a slightly latter TS than that obtained *in vacuo.* As in the case of **TS*β*a**, the Becke3LYP functional yields a C(2)−C(3) distance larger than that found at RHF level. We tried to optimize the structure of **TS*δ*a** at CASSCF/3−21G level, as we did for **TS*β*a**. We explored extensively the CASSCF(2,2)/3−21G and CASSCF(4,4)/3−21G potential energy hypersurfaces. In all cases, our attempts were unsuccessful. They always led to structures close to either **TS*β*a**, the zwitterionic intermediates, or the products.

The energies of **TS*β*a** and **TS*δ*a** are collected in Table 1. With the exception of the CASSCF result, all the levels included in Table 1 predict preferential formation of *δ*-lactam **4a**, both in the gas phase and in solution. Thus, at the HF/6−31G* level **TS*δ*a** is predicted to be 2.28 kcal/mol lower in energy than **TS*β*a**, the corresponding value at HF/(SCRF)/6−31G* level being 1.84 kcal/mol. At Becke3LYP and MP2 levels, this energy gap is higher, although the SCRF value at this latter level is *ca.* 0.5 kcal/mol lower than that calculated *in vacuo.* The energies of both TS's are closer as the Møller−Plesset expansion develops, and the MP4SDQ/6−31G* energy turns out to be quite similar to that obtained *in vacuo* at the HF/6−31G* level. However, all these data seem to suggest that the [4 + 2] cycloadduct **4a** is obtained, whereas the CASSCF method predicts the exclusive formation of the [2 + 2] cycloadduct **3a**, in agreement with the experimental results obtained by Kato *et al.*[49] However, it should be emphasized that these authors reported that ketene **1a** is quite unreactive toward α,*β*-unsaturated imines and that the cycloaddition must be carried out at 180−200 °C. In Table 2 we have reported the zero-point vibrational energies, the vibrational enthalpies, and the entropies of **TS*β*a** and **TS*δ*a**, computed

(52) (a) Dewar, M. J. S.; Olivella, S.; Stewart, J. J. P. *J. Am. Chem. Soc.* **1986**, *108*, 5771. (b) Dannenberg, J. J.; Tanaka, K. *J. Am. Chem. Soc.* **1985**, *107*, 671. (c) Dewar, M. J. S.; Jie, C. *J. Am. Chem. Soc.* **1987**, *109*, 5893.

(53) Schmidt, M. W.; Nguyen, K. A.; Gordon, M. S.; Montgomery, J. A. *J. Am. Chem. Soc.* **1991**, *113*, 5998.

(54) In line with this result, the Mulliken Charges for the C(3) and C(4) atoms are higher at the HF/3-21G level than at the CASSCF-(2,2)/3−21G level. Similarly, the dipole moments of **TS*β*a** at the HF/3−21G and CASSCF/3−21G levels are 2.466 and 1.470 D, respectively.

Table 1. Total Energies (au) and Relative Energies (kcal/mol) of the Transition Structures TSβa and TSδa, Leading to Cycloadducts 3a and 4a, Respectively

method	TSβa	TSδa
	$\epsilon = 1.00$	
HF/3-21G	−320.777 67 (0.00)	−320.782 21 (−2.85)
HF/6-31G*	−322.579 61 (0.00)	−322.583 25 (−2.28)
Becke3LYP/6-31G*	−324.602 33 (0.00)	−324.609 58 (−4.55)
MP2/6-31G*//HF/6-31G*	−323.564 65 (0.00)	−323.570 95 (−3.95)
MP3/6-31G*//HF/6-31G*	−323.588 32 (0.00)	−323.592 98 (−2.92)
MP4SDQ/6-31G*//HF/6-31G*	−323.607 06 (0.00)	−323.610 76 (−2.32)
CASSCF(2,2)/3-21G	−320.829 64	
	$\epsilon = 9.08$	
HF/3-21G	−320.785 34 (0.00)	−320.789 45(−2.58)
HF/6-31G*	−322.587 29 (0.00)	−322.590 23(−1.84)
MP2/6-31G*//HF/6-31G*	−323.570 13 (0.00)	−323.575 65(−3.46)

Table 2. Zero-Point Vibrational Energies (ZPVE, kcal/mol), Vibrational Enthalpies (H^T_{vib}, kcal/mol), and Total Entropies (S^T, cal/K·mol) Corresponding to Transition Structures TSβa and TSδa

species	ZPVE	H^{298}_{vib}	H^{473}_{vib}	S^{298}	S^{473}
			$\epsilon = 1.00$		
TSβa	74.61	78.71	83.79	81.84	95.96
TSδa	75.32	79.16	84.14	78.76	92.61
			$\epsilon = 9.08$		
TSβa	74.62	78.71	83.79	80.89	95.00
TSδa	75.49	79.30	84.24	78.60	92.35

[a] All quantities have been computed on HF/6-31G* and HF-(SCRF)/6-31G* wave functions and geometries.

at 298 and 473 K with the HF/6−31G* wave functions and geometries, both in the gas phase and in solution. The results included in Table 2 indicate that the ZPVE's and vibrational enthalpies of **TSδa** are higher than those of **TSβa**, whereas the total entropies are lower. These differences in enthalpy and entropy are enhanced at 473 K. Considering the free energy differences in both TS's at the HF/6−31G*+ΔZPVE+ΔH^{473}_{vib}+ΔS^{473} or MP4SDQ/6−31G*//HF/6−31G*+ΔZPVE+ΔH^{473}_{vib} +ΔS^{473} levels, we can see that **TSβa** is 0.61 and 0.57 kcal/mol lower in energy than **TSδa**, respectively, the favorable free energy balance for **TSβa** being 0.81 kcal/mol in solution at the former level. Therefore, if the thermal and solvent effects operating under experimental conditions are taken into account, the monoreference methods do also predict preferential formation of β-lactam **3a**.

Once we have studied the interaction between ketene and (*E*)-1-azabutadiene **2a**, we turned our attention to monosubstituted ketenes such as hydroxyketene (**1b**) (as a simple model for alkoxyketenes like methoxyketene (**1c**) and chloroketene (**1d**). These two cumulenes are much more reactive than ketene itself, and they suffer the nucleophilic attack even at −78 °C (see the Experimental Section). As a consequence, it is expected that thermal factors are not relevant in the periselectivity of ketenes **1b**−**d** toward α,β-unsaturated imines. We have located eight transition structures **TSβb**−**e** and **TSδb**−**e** corresponding to the ring closure step associated to formation of [2 + 2] cycloadducts **3b**−**e** and [4 + 2] cycloadducts **4b**−**e**. The chief geometrical features of these transition structures are depicted in Figure 4 and in Figure 2 of the supporting information. The energies of all these transition structures are collected in Tables 2 and 3 of the supporting information. It is readily seen from these data that MP2/6−31G*//HF/3−21G (see Figure 4) and CASSCF(2,2)/6−31G*//HF/3−21G energies predict that saddle points **TSβb** and **TSβd** have the lowest energies. Notice that these transition structures lead to formation

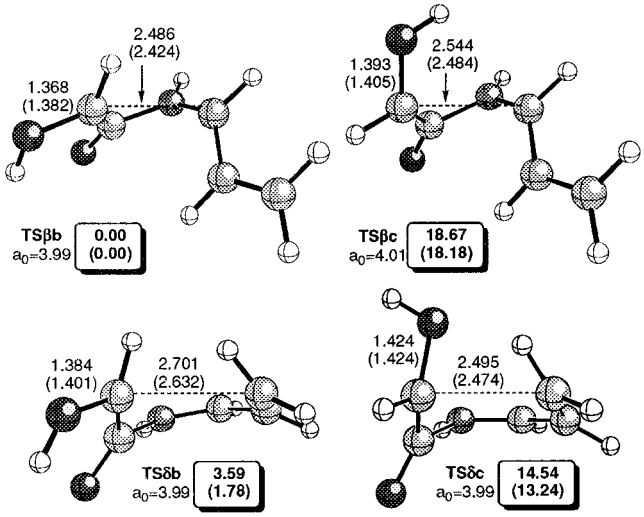

Figure 4. Computer plots of fully optimized saddle points **TSβb,c** and **TSδb,c**, calculated at the HF/3-21G and HF-(SCRF)/3-21G (in parentheses) levels. Bold numbers correspond to the relative energies (in kcal/mol) computed at the MP2/6-31G*//HF/3-21G and MP2(SCRF)/6-31G*//HF(SCRF)/3-21G levels.

of the *cis*-β-lactams **3b** and **3d**, respectively, in good agreement with experimental evidence (*vide supra*). It is also noteworthy that the differences in energy between *3-inward* and *3-outward* transition structures are much higher in **TSβb,d** than in **TSδb,d**. This result indicates that torquoelectronic effects are more important in **TSβ** transition structures than in their **TSδ** analogs. This effect is readily explained taking into account the four-electron interaction between a filled orbital of *3-inward* donor and the C(3)· · ·C(4) bond in formation. This destabilizing effect is more important in conrotatory saddle points because of the higher overlap between both systems (see Figure 5). During the course of this work, Houk *et al.*[55] have reported an *ab initio* study on torquoelectronic effects in disrotatory pericyclic reactions of substituted 1,3,5-hexatrienes. These authors have also concluded that six-electron transition structures of pericyclic reactions are less sensitive to torquoelectronic effects than four-electron transition structures.

We have also studied the behavior of chloromethylketene (**1e**). Figure 6 depicts the chief geometrical features of transition structures **TSβf,g** and **TSδf,g**, corresponding to the interaction between **1e** and **2a** to form lactams **3f,g** and **4f,g**, respectively. In this case,

(55) Evanseck, J. D.; Thomas IV, B. E.; Spellmeyer, D. C.; Houk, K. N. *J. Org. Chem.* **1995**, *60*, 7134.

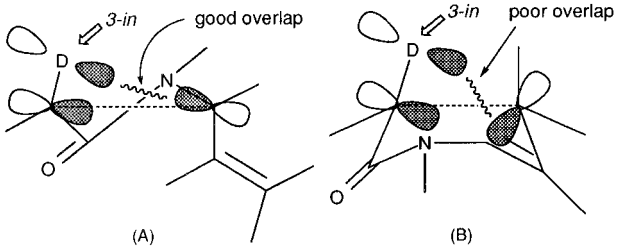

Figure 5. Schematic representation of the four-electron interaction between a filled orbital of a *3-inward* substituent and the C(3)···C(4) bond in the formation in **TS*β*** (left) and **TS*δ*** (right) saddle points.

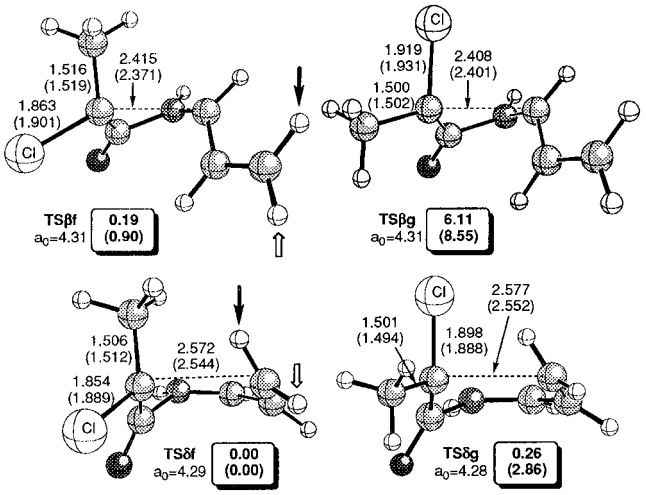

Figure 6. Computer plots of fully optimized saddle points **TS*βf,g*** and **TS*δf,g***, calculated at the HF/3-21G and HF-(SCRF)/3-21G (in parentheses) levels. Bold numbers correspond to the relative energies (in kcal/mol) computed at the MP2/6-31G*//HF/3-21G and MP2(SCRF)/6-31G*//HF(SCRF)/3-21G levels.

all transition structures must necessarily incorporate *3-inward* donors. The energies of these four transition structures have been collected in Table 4 of the supporting information. Our results indicate that **TS*δ*f** leading to *δ*-lactam **4f**, in which the methyl group and the methinic C(4)H proton are in a *cis* relationship, is the less energetic saddle point. The closest transition structure is **TS*β*f**, in which the methyl group is also occupying the *3-inward* position. This latter structure is predicted to be only 0.19 and 0.90 kcal/mol higher in energy than **TS*δ*f** at MP2/6−31G*//HF/3−21G and MP2(SCRF)/6−31G*//HF(SCRF)/3−21G levels, respectively (see Figure 6). The preference for the TSs which incorporate *3-inward* methyl groups can be explained by taking into account the four-electron interaction depicted in Figure 5. According to this Figure 5, the lone pairs of chlorine act as stronger donors than the filled *π*-orbitals of the methyl group.[56] Therefore, our results indicate that stereocontrol is more effective than pericontrol for this kind of reaction. In fact, it is found experimentally that reaction of chloro methylketene with α,*β*-unsaturated imines yields exclusively *δ*-lactams such as **4q** or

(56) It should be noted that, although the *σ* and *σ*$^+$ terms of chlorine are positive whereas those of methyl are negative, the *σ*°$_R$ parameters for chlorine and methyl are −0.21 and −0.10, respectively. Therefore, the resonance terms, more relevant in this case, suggest that chlorine is a better donor than methyl if inductive effects are not considered. See: Isaacs, N. L. *Physical Organic Chemistry*; Longman: Essex, 1987; p 158 and references therein.

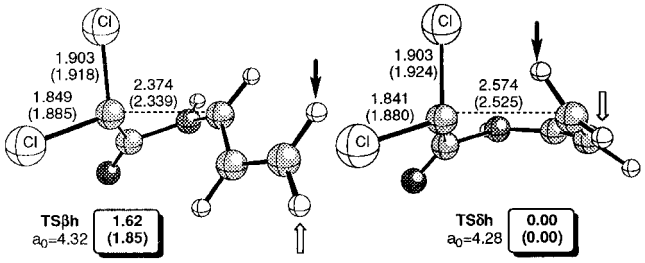

Figure 7. Computer plots of fully optimized saddle points **TS*β*h** and **TS*δ*h**, calculated at the HF/3-21G and HF(SCRF)/3-21G (in parentheses) levels. Bold numbers correspond to the relative energies (in kcal/mol) computed at the MP2/6-31G*//HF/3-21G and MP2(SCRF)/6-31G*//HF(SCRF)/3-21G levels.

mixtures of *cis*-*β*- and *cis*-*δ*-lactams as indicated in Scheme 3.

To conclude our investigation on the substituent effects in the ketene moiety, we studied the interaction between dichloroketene (**1f**) and **2a.** The geometries of the transition structures **TS*β*h** and **TS*δ*h**, both in the gas phase and in solution, are depicted in Figure 7. The corresponding energies at different theoretical levels are reported in Table 5 of the supporting information. In this case, there is necessarily a chlorine atom in a *3-inward* disposition, and therefore, the torquoelectronic destabilization induced by this atom must be higher in **TS*β*h** than in **TS*δ*h**. From our results, we can observe, as anticipated, that the preference of **TS*δ*h** over **TS*β*h** is higher than in the preceding case. Thus, the latter saddle point is calculated to be 1.62 kcal/mol higher in energy than the former at MP2/6−31G* level (*in vacuo* results, see Table 5 of the supporting information). It is noteworthy that in this case the CASSCF method again predicts incorrectly the preferential formation of the [2 + 2] cycloadducts, a result similar to that found in the TSs considered in Table 4 of the supporting information. From these data it is clear that the CASSCF(2,2) method overestimates the biradical character of **TS*β*** transition structures, predicting monotonously exclusive formation of [2 + 2] cycloadducts.[57]

We have also indicated, by means of hollow arrows in Figures 6 and 7, the position occupied by substituents derived from (*E*)-olefinic moieties in the starting α,*β*-unsaturated imines. From Figures 6 and 7 it is clear that these substituents do not affect significantly (at least from a steric viewpoint) the relative stability of the corresponding **TS*β*** and **TS*δ*** saddle points. However, a *β*-disubstituted imine or a (*Z*)-olefinic moiety should accommodate a bulky substituent in the *4-inward* position of **TS*δ*h** (marked in Figures 6 and 7 as black arrows). Given the low torsion around the C(4) and C(5) atoms in these disrotatory transition structures, this leads to a high steric congestion. Since this effect has no consequences in the alternative **TS*β*** transition structures, the latter saddle points will be the preferred ones. This analysis explains the exclusive formation of *β*-lactams in the reaction between dichloroketene and 4,4-diphenyl-1-azadienes[20] and in the reaction of ketene **1e** and imine **2′b** (*vide supra*).

Conclusions

The following conclusions can be drawn from the results discussed in this work: (i) The Staudinger reac-

(57) For a high-level computational treatment of this problem, see: Kozlowski, P.M.; Dupuis, M.; Davidson, E. R. *J. Am. Chem. Soc.* **1995**, *117*, 774.

tion between ketene and α,*β*-unsaturated imines leads to the preferential formation of [2 + 2] cycloadducts (*β*-lactams) because solvent, vibrational, thermal, and entropic factors favor the conrotatory transition structure. (ii) Monosubstituted activated ketenes form exclusively *cis*-*β*-lactams. This result can be rationalized in terms of the lower energy of the conrotatory transition structures which incorporate the donors in the *3-outward* position, the vinylic moiety being *4-inward*. (iii) Disubstituted ketenes exhibit low to high periselectivity depending on the nature of the substituents of the imine and the ketene. In general, a preference for the [4 + 2] cycloadduct is observed because of the relatively low sensitivity of the disrotatory transition structures **TS*δ*** toward torquoelectronic effects. (iv) The periselectivity of the reaction is very sensitive to the *β*-substitution in the α,*β*-unsaturated imine, since the *4-inward* position of the disrotatory **TS*δ*** transition structure is sterically very demanding.

Experimental Section

General. Commercially available compounds were used as purchased without further purification. All solvents were anhydrized and distilled according to standard protocols.[58]

The glassware used in the cycloaddition reactions was oven or flame dried and assembled under a slightly positive argon pressure. Melting points are uncorrected. Chemical shifts in the ^{1}H-NMR spectra are reported as δ values (ppm) relative to internal hexamethyldisiloxane (δ = 0.055 ppm). The nuclear Overhauser effect (NOE) experiments were run at 300 MHz by preirradiating the desired signals for 15 s with the decoupler channel turned on at 15 db below 1 W and acquiring the spectrum with the decoupler turned off. The enhancements were directly measured by integration of the signals resulting from the respective difference spectra.

General Procedures for Cycloaddition Reactions. Method A. To a stirred solution of the corresponding imine **2** (10 mmol) and triethylamine (2.1 mL, 15 mmol) in dichloromethane (20 mL) was added a solution of acyl chloride **1′** (10 mmol) in the same solvent (5 mL) dropwise at −78 °C under argon atmosphere. The reaction mixture was stirred for 14 h, during which time the temperature was allowed to reach room temperature. The resulting mixture was poured into water (25 mL), washed with 1 N HCl (25 mL) and saturated solution of $NaHCO_3$ (25 mL), and dried over Na_2SO_4. Evaporation of the solvent under reduced pressure gave a residue, which was purified by flash chromatography (silica gel, 70−230 mesh, ethyl acetate/hexanes 1:20 as eluent).

Method B. To a cooled (−78 °C) and stirred solution of acyl chloride **1′** (10 mmol) in dichloromethane (80 mL) was added dropwise a solution of triethylamine (2.1 mL) in the same solvent (20 mL) under argon atmosphere. Then, a solution of the imine **2** (10 mmol) in dichloromethane (25 mL) was added dropwise for 30 min at −78 °C. The reaction mixture was stirred for 14 h during which time the mixture was allowed to reach room temperature. The workup described in method A yielded a residue which was purified by flash chromatography (silica gel 70−230 mesh, ethyl acetate/hexanes 1:20 as eluent).

***cis*-3-Methoxy-1-methyl-4-[(*E*)-α-methylstyryl]azetidin-2-one (3i)** was prepared from imine **2b** and methoxyacetyl chloride (**1′c**), following method A: yield 56%; colorless oil; IR (film) 1753 cm^{-1}; ^{1}H-NMR ($CDCl_3$) δ 7.37−7.25 (m, 5H), 6.53 (s_{br}, 1H), 4.65 (d, 1H, J = 4.6 Hz), 4.23 (d, 1H, J = 4.6 Hz), 3.47 (s, 3H), 2.84 (s, 3H), 1.93 (d, 3H, J = 1.4 Hz); ^{13}C-NMR ($CDCl_3$) δ 167.3, 136.6, 132.6, 130.0, 128.8, 128.0, 126.7, 85.9, 66.5, 58.6, 26.7, 14.8.

***cis*-3-Methoxy-1-methyl-4-[(*Z*)-α-methylstyryl]azetidin-2-one (3′i)** was prepared from imine **2′b** and methoxyacetyl chloride (**1′c**), following method A: yield 61%; colorless oil; IR (film) 1754 cm^{-1}; ^{1}H-NMR ($CDCl_3$) δ 7.36−7.14 (m, 5H), 6.75 (S_{br}, 1H) 4.63 (s, 2H), 3.57 (s_{br}, 3H), 2.74 (s, 3H), 1.95 (d, 3H); ^{13}C-NMR ($CDCl_3$) δ 167.2, 136.2, 133.3, 132.0, 128.3, 128.0, 126.7, 86.3, 59.5, 58.8, 27.0, 20.0.

***cis*-3-Methoxy-1-methyl-4-[(*E*)-α-phenylstyryl]azetidin-2-one (3k)** was prepared from imine **2c** and methoxyacetyl chloride (**1′c**), following method A: yield 64%; colorless crystals (needles); mp 102−103 °C (from ethyl acetate in hexanes); IR (KBr) 1766 cm^{-1}; ^{1}H-NMR ($CDCl_3$) δ 7.34−6.99 (m, 10H), 6.56 (s_{br}, 1H), 4.62 (d, 1H, J = 4.6Hz), 4.50(dd, 1H, J = 4.6Hz, J' = 1Hz), 3.41 (s, 3H), 2.88 (s, 3H); ^{13}C-NMR ($CDCl_3$) δ 167.4, 138.6, 135.8, 134.8, 129.2, 129.1, 129.0, 128.6, 127.8, 127.5, 126.9, 88.3, 65.6, 59.1, 26.8. Anal. Calcd for $C_{19}H_{19}O_2N$: C, 77.77; H, 6.54; N, 4.78. Found: C, 77.92; H, 6.64; N, 4.72.

***cis*-3-Methoxy-1-methyl-4-[(*Z*)-α-phenylstyryl]azetidin-2-one (3′k)** was prepared from imine **2′c** and methoxyacetyl chloride (**1′c**), following method A: yield 54%; colorless oil; IR (film) 1755 cm^{-1}; ^{1}H-NMR ($CDCl_3$) δ 7.56−7.26 (m, 10H), 6.97 (s_{br}, 1H), 4.86 (dd, 1H, J = 4.8 Hz, J' = 0.8 Hz), 4.79 (d, 1H, J = 4.8 Hz), 3.72 (s, 3H), 2.23 (s, 3H); ^{13}C-NMR ($CDCl_3$) δ 167.2, 140.0, 137.7, 136.3, 134.6, 128.7, 128.5, 128.4, 128.3, 127.6, 127.4, 87.4, 60.9, 59.4, 26.9.

***cis*-3-Chloro-1-methyl-4-[(*E*)-α-methylstyryl]azetidin-2-one (3m)** was prepared from imine **2b** and chloroacetyl chloride (**1′d**), following method A: yield 40%; yellow oil; IR (film) 1764 cm^{-1}; ^{1}H-NMR ($CDCl_3$) δ 7.37−7.26 (m, 5H), 6.48 (s_{br}, 1H), 5.04 (d, 1H, J = 4.7Hz), 4.38 (d, 1H, J = 4.7Hz), 2.93 (s, 3H), 1.89 (s, 3H); ^{13}C-NMR ($CDCl_3$) δ 164.3, 136.4, 130.9, 129.7, 128.9, 128.2, 127.0, 64.9, 60.4, 28.0, 15.8.

***cis*-3-Chloro-1,3-dimethyl-4,5-diphenyl-3,4-dihydro-2-pyridone (4q)** was prepared from imine **2c** and and 2-chloropropionyl chloride **1′e,** following method A: yield 90%; yellow crystals: mp 131−132 °C (from ethanol); IR (KBr) 1674cm^{-1}; ^{1}H-NMR ($CDCl_3$) δ 7.28−7.16 (m, 10H), 6.63 (s, 1H), 4.15 (s, 1H), 3.33 (s, 3H), 1.57 (s, 3H); ^{13}C-NMR ($CDCl_3$) δ 166.0, 137.5, 136.3, 129.2, 128.6, 128.2, 127.1, 126.4, 125.0, 121.8, 66.3, 57.1, 35.2, 25.0. Anal. Calcd for $C_{19}H_{18}ONCl$: C, 73.18; H, 5.83; N, 4.49. Found: C, 72.92; H, 5.77; N, 4.37.

***cis*-3-Chloro-4-phenyl-1,3,5-trimethyl-3,4-dihydro-2--pyridone (4o** was prepared from imine **2b** and and 2-chloropropionyl chloride (**1′e**), following method B: yield 7%; colorless crystals: mp 72−73 °C (from ethyl acetate in hexanes); IR (KBr) 1672 cm^{-1}; ^{1}H-NMR ($CDCl_3$) δ 7.28−7.02 (m, 5H), 5.98 (d, 1H, J = 1.5 Hz), 3.47 (s, 1H), 3.20 (s, 3H), 1.69 (d, 3H, J = 1.5Hz), 1.48 (s, 3H); ^{13}C-NMR ($CDCl_3$) δ 165.8, 136.6, 129.0, 128.1, 128.0, 124.4, 118.8, 66.5, 59.3, 34.8, 25.0, 18.7. Anal. Calcd for $C_{14}H_{16}ONCl$: C, 67.31; H, 6.47; N, 5.61. Found: C, 67.22; H, 6.49; N, 5.54.

***cis*-3-Chloro-1,3-dimethyl-4-[(*E*)-α-methylstyryl]azetidin-2-one (3o)** was prepared from imine **2b** and 2-chloropropionyl chloride (**1′e**), following method B: yield 16%; colorless oil; IR (film) 1771 cm^{-1}; ^{1}H-NMR ($CDCl_3$) δ 7.40−7.26 (m, 5H), 6.43 (s_{br}, 1H), 4.06 (s, 1H), 2.94 (s, 3H), 1.91 (d, 3H, J = 1Hz), 1.89 (s, 3H); ^{13}C-NMR ($CDCl_3$) δ 167.2, 136.5, 131.8, 129.0, 128.5, 128.2, 127.0, 73.6, 72.3, 28.0, 24.8, 16.1.

***cis*-3-Chloro-1,3-dimethyl-4-[(*Z*)-α-methylstyryl]azetidin-2-one (3′o)** was prepared from imine **2′b** and 2-chloropropionyl chloride (**1′e**), following method B: yield 6%; colorless oil; IR(film) 1771 cm^{-1}; ^{1}H-NMR ($CDCl_3$) δ 7.37−7.11 (m, 5H), 6.87 (s_{br}, 1H), 4.28 (s_{br}, 1H), 2.78 (s, 3H), 1.95 (d, 3H, J = 1.5Hz), 1.82 (s, 3H); ^{13}C-NMR ($CDCl_3$) δ 167.2, 136.3, 133.7, 133.2, 128.7, 128.1, 127.3, 72.3, 67.3, 29.6, 28.3, 24.6.

(3*S,4*S**,5*S**,6*S**)-3-Chloro-5-formyl-1,3,5-trimethyl-6-[(E)-α-methylstyryl]piperidin-2-one (6)** was prepared from imine **2b** and 2-chloropropionyl chloride (**1′e**), following method A: yield 41%; white crystals; mp 55−56 °C (from ethyl acetate in hexanes); IR (KBr) 1722, 1655 cm^{-1}; ^{1}H-NMR ($CDCl_3$) δ 9.22 (s, 1H), 7.48−7.26 (m, 10H), 6.43 (s, 1H), 4.11 (s, 1H), 3.83 (s, 1H), 3.02 (s, 3H), 1.89 (s, 3H), 1.88 (s, 3H), 1.78 (s, 3H); ^{13}C-NMR ($CDCl_3$) δ 201.2, 168.7, 135.7, 134.6, 131.8, 131.7, 129.2, 129.1, 128.5, 128.4, 127.7, 75.8, 65.9, 51.4, 50.2, 35.6, 29.7, 18.8,

(58) Perrin, D. D.; Armarego, W. L. F. *Purification of Laboratory Chemicals*; Pergamon: Oxford, 1988.

18.2. Anal. Calcd for $C_{24}H_{26}O_2NCl$: C, 72.80; H, 6.63; N, 3.54. Found: C, 72.79; H, 6.56; N, 3.47.[59]

Acknowledgment. This work has been supported by the Universidad del País Vasco-Euskal Herriko Unibertsitatea (Project UPV 170.215-EA156/94), by the Gobierno Vasco-Eusko Jaurlaritza (Project GV 170.215−0119/94), and by Diputación Foral de Gipuzkoa-Gipuzkoako Foru Aldundia (Project 0733/94). Two grants to I.A. and G.R. from the Gobierno Vasco-Eusko Jaurlaritza and Ministerio de Educación y Ciencia are gratefully acknowledged. We thank the Plan Nacional de I+D (CICYT) and the CIEMAT for a generous gift of computing time at the CRAY YMP-EL computer.

Supporting Information Available: Additional experimental details and characterization of imines **2b**,**c** and compounds, **5i**,**k**; Cartesian coordinates of optimized geometries of saddle points **TS*β*a**−**h** and **TS*δ*a**−**h**; tables including the total energies at different theoretical levels of the transition structures discussed in the text; ball and stick representations of the X-ray structure of compound **6** and **TSb**−**e** (32 pages). This material is contained in libraries on microfiche, immediately follows this article in the microfilm version of the journal, and can be ordered from the ACS; see any current masthead page for ordering information.

JO951867W

(59) The author has deposited atomic coordinates for **6** with the Cambridge Crystallographic Data Centre. The coordinates can be obtained, on request, from the Director, Cambridge Crystallographic Data Centre, 12 Union Road, Cambridge, CB2 1EZ, UK.